AIAA JOURNAL
Vol. 40, No. 2, February 2002

Model Reduction for Dynamical Systems with Local Nonlinearities

Zu-Qing Qu*
Shanghai Jiao Tong University, 200030 Shanghai, People's Republic of China

Many kinds of nonlinear engineering systems have a large number of degrees of freedom while nonlinear components are spatially localized. Even though the local nonlinearities constitute only a small part of the system, the dynamic behavior of the system is wholly nonlinear, and the analysis of the whole model is very expensive. To reduce the computational effort significantly, two model reduction schemes are proposed to reduce the size of the nonlinear model before the analysis is performed. One is defined on the system level, and the other is on the substructure level. They are both based on the dynamic condensation technique. In the former scheme the dynamic condensation technique is implemented into the linear part of the whole system directly, whereas it is applied to the linear flexible substructures in the later scheme. The accuracy and stability of the former is usually better than the latter. However, it is more computationally expensive than the latter. Two numerical examples are also included. The results show that the present two schemes are feasible and efficient to reduce the degrees of freedom of the model with local nonlinearities.

Nomenclature

$\boldsymbol{C}$	=	$(n \times n)$ damping matrix of the full model
$\boldsymbol{C}_R^{(0)}$	=	$(n_k \times n_k)$ initially or statically approximate damping matrix of the reduced model
$\boldsymbol{F}$	=	external force vector acting on the system
$\boldsymbol{F}_R^{(0)}$	=	initially or statically approximate external force vector of the reduced model
$\boldsymbol{G}(\boldsymbol{X})$	=	nonlinear force vector
$\boldsymbol{I}$	=	$(n_k \times n_k)$ identity matrix
$\boldsymbol{K}$	=	$(n \times n)$ stiffness matrix of the full model
$\boldsymbol{K}^L$	=	$(n \times n)$ linear stiffness matrix of the full model with local nonlinearities
$\boldsymbol{K}^N$	=	$(n \times n)$ nonlinear stiffness matrix of the full model with local nonlinearities
$\boldsymbol{K}_R^{(0)}$	=	$(n_k \times n_k)$ initially or statically approximate stiffness matrix of the reduced model
$\boldsymbol{M}$	=	$(n \times n)$ mass matrix of the full model
$\boldsymbol{M}_R^{(0)}$	=	$(n_k \times n_k)$ initially or statically approximate mass matrix of the reduced model
n	=	number of total degrees of freedom of the full model
$\boldsymbol{R}$	=	$(n_d \times n_k)$ dynamic condensation matrix
$\boldsymbol{T}$	=	$(n \times n_k)$ coordinate transformation matrix
$\boldsymbol{X}$	=	displacement response vector
$\dot{\boldsymbol{X}}$	=	velocity response vector
$\ddot{\boldsymbol{X}}$	=	acceleration response vector
φ_r	=	rigid mode shape of the substructure

Subscripts

d	=	parameters associated with the deleted degrees of freedom
k	=	parameters associated with the kept degrees of freedom
R	=	parameters associated with the reduced model

Superscripts

$i, i+1$	=	ith and $(i+1)$th approximation
L	=	linear stiffness matrix
N	=	nonlinear stiffness matrix
T	=	matrix transpose
0	=	initial or static approximation

Introduction

THERE are many kinds of nonlinear engineering systems that have a large number of degrees of freedom (DOFs), but nonlinear components are spatially localized. Examples of such systems are rotating mechanical systems with nonlinear bearing supports, mechanical systems with dry friction and backlash phenomena in certain connections, vibration control systems with local nonlinear springs and/or dampers, etc. From a spatial point of view, although the local nonlinearities constitute only a small part of the mechanical system the dynamic behavior of the system is wholly nonlinear. The numerical analysis of the dynamic behavior of these kinds of models generally needs much computing time and can cause computational problems. How to treat such kinds of systems is an important problem for nonlinear analysis.[1]

The simplest method is directly to solve the large order of dynamic model using direct integration with iteration in time domain. Obviously, this method is very computationally expensive. Recently, several reduction methods have been proposed to solve this problem. In these methods the nonlinear equations of motion are transformed into a set of condensed simultaneous nonlinear algebraic equations. If the number of these coordinates is very small compared to that of the entire system, a substantial reduction of computational work will be expected.

Fey et al.[2] studied the long-term behavior of the mechanical system with local nonlinearity using component mode synthesis technique. This method was also used by Nataraj and Nelson.[3] A modal transformation method was used by Zheng and Hasebe[1] to reduce the number of degrees of freedom of linear subset. These works not only save computing time but also avoid the convergence difficulty in numerical calculation. However, the reduced models obtained from these methods are defined in general coordinates or modal coordinates, and the calculation of the eigenvalues and egenvectors are required before using these approaches.

Rouch and Kao[4] employed Guyan/static[5] reduction method to arrive at a reduced size model. Mclean and Hahn[6] proposed a solution technique with a static reduction to evaluate the response of the system. Shiau and Jean[7] developed a reduction technique, which is similar to Guyan reduction, to link the harmonic balance method for investigating the periodic synchronous and nonsynchronous response of large-order nonlinear rotor dynamic systems.

Received 29 March 2001; revision received 14 July 2001; accepted for publication 18 July 2001.

*Professor, State Key Laboratory of Vibration, Shock and Noise; currently Research Associate, Department of Civil Engineering, University of Arkansas, 4190 Bell Engineering Center, Fayetteville, AR 72701; qu@engr.uark.edu. Member AIAA.

As we know the inertia terms are ignored in Guyan reduction, the reduced model obtained from this method is only exact for static problems. For dynamic problems the accuracy is usually very low and deeply dependent on the selection of the kept DOFs. Improperly kept DOFs or an insufficient number of them would result in serious errors.

To improve the accuracy of the reduced model resulted from Guyan reduction, the iterative scheme proposed by the author[8] recently will be used in this paper. Two schemes for the model reduction of nonlinear models will be proposed. They are defined on the system and the substructure levels, respectively. Two numerical examples, a beam-spring system and a floating raft isolation system, are included to demonstrate the implementation of the proposed approaches.

Dynamic Condensation Method

The dynamic equilibrium of a system with n DOFs is given by

$$\boldsymbol{M}\ddot{\boldsymbol{X}} + \boldsymbol{C}\dot{\boldsymbol{X}} + \boldsymbol{K}\boldsymbol{X} = \boldsymbol{F} \tag{1}$$

The damping matrix $\boldsymbol{C}$ in Eq. (1) is usually assumed to be proportional to the mass and/or stiffness matrices for structures, that is,

$$\boldsymbol{C} = \alpha\boldsymbol{M} + \beta\boldsymbol{K} \tag{2}$$

α and β are constants. If the total DOFs of the full model are divided into the kept and deleted DOFs, Eq. (1) can be rearranged in a partitioned form as

$$\begin{bmatrix} \boldsymbol{M}_{kk} & \boldsymbol{M}_{kd} \\ \boldsymbol{M}_{dk} & \boldsymbol{M}_{dd} \end{bmatrix} \begin{Bmatrix} \ddot{\boldsymbol{X}}_k \\ \ddot{\boldsymbol{X}}_d \end{Bmatrix} + \begin{bmatrix} \boldsymbol{C}_{kk} & \boldsymbol{C}_{kd} \\ \boldsymbol{C}_{dk} & \boldsymbol{C}_{dd} \end{bmatrix} \begin{Bmatrix} \dot{\boldsymbol{X}}_k \\ \dot{\boldsymbol{X}}_d \end{Bmatrix} + \begin{bmatrix} \boldsymbol{K}_{kk} & \boldsymbol{K}_{kd} \\ \boldsymbol{K}_{dk} & \boldsymbol{K}_{dd} \end{bmatrix} \begin{Bmatrix} \boldsymbol{X}_k \\ \boldsymbol{X}_d \end{Bmatrix} = \begin{Bmatrix} \boldsymbol{F}_k \\ \boldsymbol{F}_d \end{Bmatrix} \tag{3}$$

Assuming the numbers of the kept and deleted DOFs are n_k and n_d, one has $n_k \ll n_d \approx n$ for a big model. Usually, the DOFs on which the dynamic characteristics (displacements, velocities, accelerations, stresses, etc.) are directly interested are required to be selected as the kept DOFs.

It can be proven[9] that the proportional damping described in Eq. (2) does not affect the dynamic condensation matrix. Also, the matrix is a natural property of the system and is independent of the external force. Therefore, the following equations are used to obtain the dynamic condensation matrix:

$$\begin{bmatrix} \boldsymbol{M}_{kk} & \boldsymbol{M}_{kd} \\ \boldsymbol{M}_{dk} & \boldsymbol{M}_{dd} \end{bmatrix} \begin{Bmatrix} \ddot{\boldsymbol{X}}_k \\ \ddot{\boldsymbol{X}}_d \end{Bmatrix} + \begin{bmatrix} \boldsymbol{K}_{kk} & \boldsymbol{K}_{kd} \\ \boldsymbol{K}_{dk} & \boldsymbol{K}_{dd} \end{bmatrix} \begin{Bmatrix} \boldsymbol{X}_k \\ \boldsymbol{X}_d \end{Bmatrix} = \begin{Bmatrix} \boldsymbol{F}_k \\ 0 \end{Bmatrix} \tag{4}$$

The second equation of Eq. (4) can be written as

$$\boldsymbol{X}_d = -\boldsymbol{K}_{dd}^{-1}(\boldsymbol{M}_{dk}\ddot{\boldsymbol{X}}_k + \boldsymbol{M}_{dd}\ddot{\boldsymbol{X}}_d + \boldsymbol{K}_{dk}\boldsymbol{X}_k) \tag{5}$$

Let $\ddot{\boldsymbol{X}}_d = 0$ and $\ddot{\boldsymbol{X}}_k = 0$ in Eq. (5), one has

$$\boldsymbol{X}_d = -\boldsymbol{K}_{dd}^{-1}\boldsymbol{K}_{dk}\boldsymbol{X}_k \equiv \boldsymbol{R}^{(0)}\boldsymbol{X}_k \tag{6}$$

The condensation matrix defined in Eq. (6) is identical to the reduction matrix in Guyan condensation method. Clearly, the inertia forces in Eq. (5) are ignored when obtaining the reduction matrix $\boldsymbol{R}^{(0)}$. Therefore, it is a static condensation, and the condensation matrix is only exact for static problems. For dynamic problems its accuracy will decrease with the increase of the natural frequencies of structures or systems.

Based on the condensation matrix $\boldsymbol{R}^{(0)}$, the dynamic equilibrium of the reduced model is given by

$$\boldsymbol{M}_R^{(0)}\ddot{\boldsymbol{X}}_k + \boldsymbol{C}_R^{(0)}\dot{\boldsymbol{X}}_k + \boldsymbol{K}_R^{(0)}\boldsymbol{X}_k = \boldsymbol{F}_R^{(0)} \tag{7}$$

where the mass matrix $\boldsymbol{M}_R^{(0)}$, stiffness matrix $\boldsymbol{K}_R^{(0)}$, and damping matrix $\boldsymbol{C}_R^{(0)}$ of the statically reduced model are defined as

$$\boldsymbol{M}_R^{(0)} = \boldsymbol{M}_{kk} + \left[\boldsymbol{R}^{(0)}\right]^T\boldsymbol{M}_{dk} + \boldsymbol{M}_{kd}\boldsymbol{R}^{(0)} + \left[\boldsymbol{R}^{(0)}\right]^T\boldsymbol{M}_{dd}\boldsymbol{R}^{(0)} \tag{8a}$$

$$\boldsymbol{K}_R^{(0)} = \boldsymbol{K}_{kk} + \left[\boldsymbol{R}^{(0)}\right]^T\boldsymbol{K}_{dk} + \boldsymbol{K}_{kd}\boldsymbol{R}^{(0)} + \left[\boldsymbol{R}^{(0)}\right]^T\boldsymbol{K}_{dd}\boldsymbol{R}^{(0)} \tag{8b}$$

$$\begin{aligned}\boldsymbol{C}_R^{(0)} &= \boldsymbol{C}_{kk} + \left[\boldsymbol{R}^{(0)}\right]^T\boldsymbol{C}_{dk} + \boldsymbol{C}_{kd}\boldsymbol{R}^{(0)} + \left[\boldsymbol{R}^{(0)}\right]^T\boldsymbol{C}_{dd}\boldsymbol{R}^{(0)} \\ &= \alpha\boldsymbol{M}_R^{(0)} + \beta\boldsymbol{K}_R^{(0)}\end{aligned} \tag{8c}$$

$\boldsymbol{F}_R^{(0)}$ is the equivalent force vector acting on the system and is given by

$$\boldsymbol{F}_R^{(0)} = \boldsymbol{F}_k \tag{9}$$

If the force vector on the deleted DOFs is not zero, the equivalent force vector becomes

$$\boldsymbol{F}_R^{(0)} = \boldsymbol{F}_k + \left[\boldsymbol{R}^{(0)}\right]^T\boldsymbol{F}_d \tag{10}$$

Research shows that the accuracy of the reduced model (8) obtained from the static reduction is usually very low and dependent on the selection of the kept DOFs. If they are selected improperly, the error is usually very big. To improve the accuracy of the reduced model, the reduction matrix $\boldsymbol{R}^{(0)}$ is modified in the following.

The free vibration of the reduced model corresponding to Eq. (7) is given by

$$\boldsymbol{M}_R^{(0)}\ddot{\boldsymbol{X}}_k + \boldsymbol{K}_R^{(0)}\boldsymbol{X}_k = 0 \tag{11}$$

which leads to

$$\ddot{\boldsymbol{X}}_k = -\left[\boldsymbol{M}_R^{(0)}\right]^{-1}\boldsymbol{K}_R^{(0)}\boldsymbol{X}_k \tag{12}$$

By differentiating both sides of Eq. (6) with respect to time twice and then using Eq. (12), one obtains

$$\ddot{\boldsymbol{X}}_d = \boldsymbol{R}^{(0)}\ddot{\boldsymbol{X}}_k = -\boldsymbol{R}^{(0)}\left[\boldsymbol{M}_R^{(0)}\right]^{-1}\boldsymbol{K}_R^{(0)}\boldsymbol{X}_k \tag{13}$$

Introducing Eqs. (12) and (13) into Eq. (5) results in

$$\boldsymbol{X}_d = \boldsymbol{K}_{dd}^{-1}\left\lfloor\left[\boldsymbol{M}_{dk} + \boldsymbol{M}_{dd}\boldsymbol{R}^{(0)}\right]\left[\boldsymbol{M}_R^{(0)}\right]^{-1}\boldsymbol{K}_R^{(0)} - \boldsymbol{K}_{dk}\right\rfloor\boldsymbol{X}_k \tag{14}$$

According to the definition of the dynamic condensation matrix $\boldsymbol{R}$ in Eq. (6), its first approximation results from Eq. (14) as

$$\boldsymbol{R}^{(1)} = \boldsymbol{K}_{dd}^{-1}\left\lfloor\left[\boldsymbol{M}_{dk} + \boldsymbol{M}_{dd}\boldsymbol{R}^{(0)}\right]\left[\boldsymbol{M}_R^{(0)}\right]^{-1}\boldsymbol{K}_R^{(0)} - \boldsymbol{K}_{dk}\right\rfloor \tag{15}$$

The first approximation of the mass matrix $\boldsymbol{M}_R^{(1)}$, stiffness matrix $\boldsymbol{K}_R^{(1)}$, and damping matrix $\boldsymbol{C}_R^{(1)}$ of the reduced model can be obtained similarly from Eq. (8) by using the dynamic condensation matrix $\boldsymbol{R}^{(1)}$. The accuracy of the matrices $\boldsymbol{K}_R^{(1)}$ and $\boldsymbol{M}_R^{(1)}$ is higher than the matrix $\boldsymbol{K}_R^{(0)}$ and $\boldsymbol{M}_R^{(0)}$ because the inertia forces are considered partially in the condensation matrix $\boldsymbol{R}^{(1)}$.

Repeating the procedure defined by Eqs. (8–15), the dynamic characteristics of the reduced model will gradually close to the full model at the low-frequency range.

Model Reduction on the System Level

Suppose the dynamic equilibrium of a nonlinear system with n DOFs can be expressed as

$$\boldsymbol{M}\ddot{\boldsymbol{X}} + \boldsymbol{C}\dot{\boldsymbol{X}} + (\boldsymbol{K}^L + \boldsymbol{K}^N)\boldsymbol{X} = \boldsymbol{F} \tag{16}$$

where the nonlinear stiffness matrix $\boldsymbol{K}^N$ is usually a function of the displacements. For convenience, Eq. (16) is sometimes rewritten as[1]

$$\boldsymbol{M}\ddot{\boldsymbol{X}} + \boldsymbol{C}\dot{\boldsymbol{X}} + \boldsymbol{K}^L\boldsymbol{X} = \boldsymbol{F} + \boldsymbol{G}(\boldsymbol{X}) \tag{17}$$

The nonlinear force vector $\boldsymbol{G}(\boldsymbol{X})$ is related to the nonlinear components of the system. It can be expressed as a nonlinear function of the displacements at positions associated with the nonlinear components, that is,

$$\boldsymbol{G}(\boldsymbol{X}) = -\boldsymbol{K}^N\boldsymbol{X} \tag{18}$$

Similarly, if the total DOFs of the full model are divided into the kept and the deleted DOFs, Eq. (16) can be partitioned as

$$\begin{bmatrix} \boldsymbol{M}_{kk} & \boldsymbol{M}_{kd} \\ \boldsymbol{M}_{dk} & \boldsymbol{M}_{dd} \end{bmatrix} \begin{Bmatrix} \ddot{\boldsymbol{X}}_k \\ \ddot{\boldsymbol{X}}_d \end{Bmatrix} + \begin{bmatrix} \boldsymbol{C}_{kk} & \boldsymbol{C}_{kd} \\ \boldsymbol{C}_{dk} & \boldsymbol{C}_{dd} \end{bmatrix} \begin{Bmatrix} \dot{\boldsymbol{X}}_k \\ \dot{\boldsymbol{X}}_d \end{Bmatrix} + \begin{bmatrix} \boldsymbol{K}_{kk}^L & \boldsymbol{K}_{kd}^L \\ \boldsymbol{K}_{dk}^L & \boldsymbol{K}_{dd}^L \end{bmatrix} \begin{Bmatrix} \boldsymbol{X}_k \\ \boldsymbol{X}_d \end{Bmatrix} + \begin{bmatrix} \boldsymbol{K}_{kk}^N & \boldsymbol{K}_{kd}^N \\ \boldsymbol{K}_{dk}^N & \boldsymbol{K}_{dd}^N \end{bmatrix} \begin{Bmatrix} \boldsymbol{X}_k \\ \boldsymbol{X}_d \end{Bmatrix} = \begin{Bmatrix} \boldsymbol{F}_k \\ \boldsymbol{F}_d \end{Bmatrix} \tag{19}$$

As shown in Eq. (6), the relation of the displacements between the kept and deleted DOFs is defined by the dynamic condensation matrix. Using this condensation matrix, the following transformation is defined:

$$\boldsymbol{X} = \begin{Bmatrix} \boldsymbol{X}_k \\ \boldsymbol{X}_d \end{Bmatrix} = \begin{Bmatrix} \boldsymbol{I} \\ \boldsymbol{R} \end{Bmatrix} \boldsymbol{X}_k = \boldsymbol{T}\boldsymbol{X}_k \tag{20}$$

where $\boldsymbol{R}$ is the dynamic condensation matrix defined in the preceding section. Because the dynamic condensation matrix is independent of time, we have

$$\begin{Bmatrix} \dot{\boldsymbol{X}}_k \\ \dot{\boldsymbol{X}}_d \end{Bmatrix} = \boldsymbol{T}\dot{\boldsymbol{X}}_k, \qquad \begin{Bmatrix} \ddot{\boldsymbol{X}}_k \\ \ddot{\boldsymbol{X}}_d \end{Bmatrix} = \boldsymbol{T}\ddot{\boldsymbol{X}}_k \tag{21}$$

Introducing Eqs. (20) and (21) into Eq. (19) and premultiplying it by the transpose of matrix $\boldsymbol{T}$ leads to

$$\boldsymbol{M}_R\ddot{\boldsymbol{X}}_k + \boldsymbol{C}_R\dot{\boldsymbol{X}}_k + \boldsymbol{K}_R^L\boldsymbol{X}_k + \boldsymbol{K}_R^N\boldsymbol{X}_k = \boldsymbol{F}_R \tag{22}$$

The reduced system matrices and force vector in Eq. (22) are defined as

$$\boldsymbol{M}_R = \boldsymbol{T}^T\boldsymbol{M}\boldsymbol{T} = \boldsymbol{M}_{\mathrm{kk}} + \boldsymbol{R}^T\boldsymbol{M}_{\mathrm{dk}} + \boldsymbol{M}_{\mathrm{kd}}\boldsymbol{R} + \boldsymbol{R}^T\boldsymbol{M}_{\mathrm{dd}}\boldsymbol{R} \tag{23a}$$

$$\boldsymbol{K}_R^L = \boldsymbol{T}^T\boldsymbol{K}^L\boldsymbol{T} = \boldsymbol{K}_{\mathrm{kk}}^L + \boldsymbol{R}^T\boldsymbol{K}_{\mathrm{dk}}^L + \boldsymbol{K}_{\mathrm{kd}}^L\boldsymbol{R} + \boldsymbol{R}^T\boldsymbol{K}_{\mathrm{dd}}^L\boldsymbol{R} \tag{23b}$$

$$\boldsymbol{C}_R = \alpha\boldsymbol{M}_R + \beta\boldsymbol{K}_R^L \tag{23c}$$

$$\boldsymbol{K}_R^N = \boldsymbol{T}^T\boldsymbol{K}^N\boldsymbol{T} = \boldsymbol{K}_{\mathrm{kk}}^N + \boldsymbol{R}^T\boldsymbol{K}_{\mathrm{dk}}^N + \boldsymbol{K}_{\mathrm{kd}}^N\boldsymbol{R} + \boldsymbol{R}^T\boldsymbol{K}_{\mathrm{dd}}^N\boldsymbol{R} \tag{23d}$$

$$\boldsymbol{F}_R = \boldsymbol{T}^T\boldsymbol{F} = \boldsymbol{F}_k + \boldsymbol{R}^T\boldsymbol{F}_d \tag{23e}$$

As just mentioned, the kept DOFs usually include those on which the dynamic characteristics are directly interested. For the nonlinear model the kept DOFs should also include those on which the nonlinear force vector $\boldsymbol{G}$ is directly dependent. Based on this selection, one has

$$\boldsymbol{K}_{\mathrm{kd}}^N = \left(\boldsymbol{K}_{\mathrm{dk}}^N\right)^T = 0, \qquad \boldsymbol{K}_{\mathrm{dd}}^N = 0 \tag{24}$$

Consequently, the nonlinear stiffness matrix of the reduced model defined in Eq. (23d) becomes

$$\boldsymbol{K}_R^N = \boldsymbol{K}_{\mathrm{kk}}^N \tag{25}$$

Equation (25) indicates that the nonlinear part of the reduced model is independent of the dynamic condensation matrix and can be obtained directly from the full model.

The main steps for the model reduction on the system level are listed here:

1) Construct the mass, damping, linear stiffness matrices, and external force vector. Construct the corresponding linear dynamic equations.

2) Compute the dynamic condensation matrix using the iterative method described in the preceding section.

3) Formulate the mass, damping, linear stiffness matrices, and force vector of the reduced model using Eq. (23).

4) Assemble the nonlinear components to construct the reduced model of the whole system. It should be noticed that the effect of the nonlinear properties on the dynamic condensation matrix is not considered. Consequently, the present approach is usually valid for the system with local nonlinearities.

Model Reduction on the Substructure Level

There are a large number of systems that consist of one or more flexible components or substructures. Several examples of these systems are machines together with their isolation system such as floating raft isolation systems,[9,10] vehicle-bridge systems,[11] rotordynamic systems,[7] etc. For these systems the finite element method is usually applied to discretize the flexible substructures at first. Then, the finite element models defined in the full spaces are assembled together with the springs, dampers, and concentrated masses to formulate the global model of the whole system. This is the most accurate modeling approach for these kinds of complex systems.

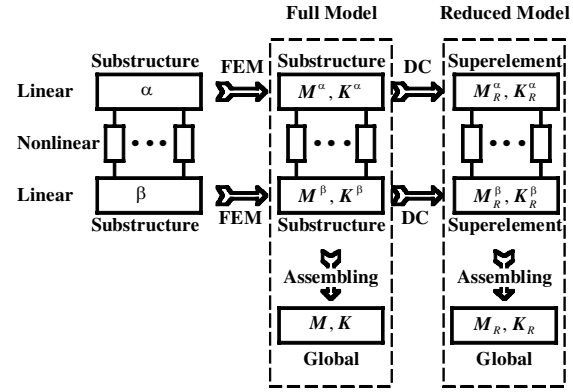

Fig. 1 Comparison of two system modeling schemes.

However, to ensure that the results have the necessary accuracy, the finite element models of these flexible substructures are usually very large.[12] This leads to a quite large final model of the whole system.

For these kinds of models, we can reduce their sizes on the substructure level. The logic of the formulation of the global model based on the full and the reduced finite element models of the substructures is shown in Fig. 1. For simplicity, only two flexible substructures are drawn in the system. The "DC" in this figure denotes dynamic condensation. From this figure we know that the sizes of the flexible substructures are reduced before the assemblage. Because only the connecting part is nonlinear, we do not need to consider the nonlinearity during the construction of the reduced model of each substructure. Assume the dynamic equations of the corresponding reduced model is

$$\tilde{\boldsymbol{M}}_R\ddot{\boldsymbol{X}}_k + \tilde{\boldsymbol{C}}_R\dot{\boldsymbol{X}}_k + \tilde{\boldsymbol{K}}_R^L\boldsymbol{X}_k + \tilde{\boldsymbol{K}}^N\boldsymbol{X}_k = \tilde{\boldsymbol{F}}_R \tag{26}$$

The main steps for the model reduction on the substructure level are as follows: 1) divide the whole system into several substructures and other components; 2) construct the system matrices for each linear flexible substructure and then formulate the corresponding reduced model using the method in the second section; and 3) assemble these reduced models and other components to formulate the reduced global model of the whole system. Because the size of the reduced model of each substructure is much smaller than the size of the corresponding full model, the total DOFs of the reduced global model are much less than that of the full global one. This idea was used by the author recently in linear models.[13]

Because the number of the DOFs of the substructures is much smaller than in the whole full model, the computation of the dynamic condensation matrix on the substructure level is much more efficient than on the system level. If there are identical substructures, the corresponding reduced models are only required to be constructed once, and, hence, much computational work can be saved. Another advantage of the model reduction on the substructure level is that we do not need to worry about the nonlinear effects because only the linear substructures are reduced. However, some information might be lost if the kept DOFs of the substructure are not selected properly.

As we know, the substructure isolated from the whole system is usually free and has rigid mode(s). It is, therefore, very important that the reduced model retains the rigid modes(s) of the full model during iterating. This will be proven in the following.

Suppose the full finite element model of a substructure has rigid modeshape(s) φ_r, that is,

$$\boldsymbol{K}\varphi_r = 0 \tag{27}$$

or in a partitioned form

$$\begin{bmatrix} \boldsymbol{K}_{\mathrm{kk}} & \boldsymbol{K}_{\mathrm{kd}} \\ \boldsymbol{K}_{\mathrm{dk}} & \boldsymbol{K}_{\mathrm{dd}} \end{bmatrix} \begin{Bmatrix} \varphi_{\mathrm{rk}} \\ \varphi_{\mathrm{rd}} \end{Bmatrix} = \begin{Bmatrix} 0 \\ 0 \end{Bmatrix} \tag{28}$$

Equation (28) is equivalent to the following two equations:

$$\boldsymbol{K}_{\mathrm{kk}}\varphi_{\mathrm{rk}} + \boldsymbol{K}_{\mathrm{kd}}\varphi_{\mathrm{rd}} = 0 \tag{29a}$$

$$\boldsymbol{K}_{\mathrm{dk}}\varphi_{\mathrm{rk}} + \boldsymbol{K}_{\mathrm{dd}}\varphi_{\mathrm{rd}} = 0 \tag{29b}$$

Equation (29b) leads to

$$\varphi_{rd} = -\boldsymbol{K}_{dd}^{-1}\boldsymbol{K}_{dk}\varphi_{rk} \tag{30}$$

Introducing Eq. (30) into Eq. (29a) results in

$$\left(\boldsymbol{K}_{kk} - \boldsymbol{K}_{kd}\boldsymbol{K}_{dd}^{-1}\boldsymbol{K}_{dk}\right)\varphi_{rk} = \boldsymbol{K}_R^{(0)}\varphi_{rk} = 0 \tag{31}$$

Equation (31) means that the reduced model obtained from the initial approximation of the dynamic condensation, Guyan condensation, can retain the rigid mode shape(s) of the full model.

The expression of the $(i+1)$th approximate dynamic condensation matrix can be similarly obtained from Eq. (15) as

$$\boldsymbol{R}^{(i+1)} = \boldsymbol{K}_{dd}^{-1}\left\lfloor\left[\boldsymbol{M}_{dk} + \boldsymbol{M}_{dd}\boldsymbol{R}^{(i)}\right]\left[\boldsymbol{M}_R^{(i)}\right]^{-1}\boldsymbol{K}_R^{(i)} - \boldsymbol{K}_{dk}\right\rfloor \tag{32}$$

For convenience, it is rewritten as

$$\boldsymbol{R}^{(i+1)} = \boldsymbol{R}^{(0)} + \Delta\boldsymbol{R}^{(i+1)} \tag{33}$$

where

$$\Delta\boldsymbol{R}^{(i+1)} = \boldsymbol{K}_{dd}^{-1}\left[\boldsymbol{M}_{dk} + \boldsymbol{M}_{dd}\boldsymbol{R}^{(i)}\right]\left[\boldsymbol{M}_R^{(i)}\right]^{-1}\boldsymbol{K}_R^{(i)} = \boldsymbol{E}^{(i)}\boldsymbol{K}_R^{(i)} \tag{34}$$

Using Eq. (33), the $(i+1)$th approximation of the stiffness matrix of the reduced model becomes

$$\begin{aligned}\boldsymbol{K}_R^{(i+1)} &= \boldsymbol{K}_{kk} + \left[\boldsymbol{R}^{(0)}\right]^T\boldsymbol{K}_{dk} + \boldsymbol{K}_{kd}\boldsymbol{R}^{(0)} + \left[\boldsymbol{R}^{(0)}\right]^T\boldsymbol{K}_{dd}\boldsymbol{R}^{(0)} \\ &+ \left[\Delta\boldsymbol{R}^{(i+1)}\right]^T\boldsymbol{K}_{dk} + \boldsymbol{K}_{kd}\Delta\boldsymbol{R}^{(i+1)} + \left[\boldsymbol{R}^{(0)}\right]^T\boldsymbol{K}_{dd}\Delta\boldsymbol{R}^{(i+1)} \\ &+ \left[\Delta\boldsymbol{R}^{(i+1)}\right]^T\boldsymbol{K}_{dd}\boldsymbol{R}^{(0)} + \left[\Delta\boldsymbol{R}^{(i+1)}\right]^T\boldsymbol{K}_{dd}\Delta\boldsymbol{R}^{(i+1)}\end{aligned} \tag{35}$$

Considering

$$\left[\boldsymbol{R}^{(0)}\right]^T\boldsymbol{K}_{dd}\Delta\boldsymbol{R}^{(i+1)} = -\boldsymbol{K}_{kd}\Delta\boldsymbol{R}^{(i+1)} \tag{36a}$$

$$\left[\Delta\boldsymbol{R}^{(i+1)}\right]^T\boldsymbol{K}_{dd}\boldsymbol{R}^{(0)} = -\left[\Delta\boldsymbol{R}^{(i+1)}\right]^T\boldsymbol{K}_{dk} \tag{36b}$$

Equation (35) can be simplified as

$$\boldsymbol{K}_R^{(i+1)} = \boldsymbol{K}_R^{(0)} + \left[\Delta\boldsymbol{R}^{(i+1)}\right]^T\boldsymbol{K}_{dd}\Delta\boldsymbol{R}^{(i+1)} \tag{37}$$

The following three steps are used to prove the conclusion:

1) For the initial approximation the stiffness matrix of the reduced model is $\boldsymbol{K}_R^{(0)}$. From Eq. (31) we know it retains the rigid mode(s) of the full model.

2) Suppose the ith approximate stiffness matrix contains the rigid mode shape(s) φ_{rk}, that is,

$$\boldsymbol{K}_R^{(i)}\varphi_{rk} = 0 \tag{38}$$

3) Let us consider the $(i+1)$th approximate stiffness matrix of the substructure. Substituting Eq. (34) into Eq. (37) results in

$$\boldsymbol{K}_R^{(i+1)} = \boldsymbol{K}_R^{(0)} + \left[\boldsymbol{K}_R^{(i)}\right]^T\left[\boldsymbol{E}^{(i)}\right]^T\boldsymbol{K}_{dd}\boldsymbol{E}^{(i)}\boldsymbol{K}_R^{(i)} \tag{39}$$

Using Eqs. (31) and (38) results in

$$\boldsymbol{K}_R^{(i+1)}\varphi_{rk} = \boldsymbol{K}_R^{(0)}\varphi_{rk} + \left[\boldsymbol{K}_R^{(i)}\right]^T\left[\boldsymbol{E}^{(i)}\right]^T\boldsymbol{K}_{dd}\boldsymbol{E}^{(i)}\boldsymbol{K}_R^{(i)}\varphi_{rk} = 0 \tag{40}$$

Equation (40) means that the $(i+1)$th approximate stiffness matrix $\boldsymbol{K}_R^{(i+1)}$ also contains the same rigid mode shape(s) of the full model.

Based on the statements 1–3, we conclude that the reduced model contains the rigid mode(s) of the full model during iterating. Therefore, the present method is still valid when the substructure is free or there is rigid mode(s) in the substructure. This conclusion was tested analytically on a three-DOF mass-stiffness system.[14]

Numerical Examples

Beam-Spring System

A simple system shown in Fig. 2 will be considered first. It consists of two identical beams connected by six springs. The properties of the two beams are total length $L = 2.0$ m, area of the cross section $A = 2.4 \times 10^{-4}$ m^2, area moment of inertia of the section $I = 8.9 \times 10^{-9}$ m^4, modulus of elasticity $E = 2.0 \times 10^{11}$ N/m^2, and mass density $\rho = 7800$ kg/m^3. The linear stiffness of the springs is $k = 2.0 \times 10^5$ N/m. Also, the six springs are assumed to be nonlinear with a cubic stiffening nonlinearity $B = 2.0 \times 10^{14}$N/m^3. This means that the spring force for an absolute displacement x is $f = kx + Bx^3$. The two beams are both discretized by the finite element method. Each beam has a total of 20 elements, 21 nodes, and 42 DOFs, as shown in Fig. 3. Therefore, the global full model has a total of 82 DOFs.

Many methods can be implemented to solve the nonlinear dynamic Eqs. (16), (22), and (26) in the frequency domain. Some typical versions are the perturbation, Ritz, Galerkin, and harmonic balance methods. The detailed information about these methods can be found from Ref. 15. The harmonic balance method is used to solve the nonlinear equations in this paper.

Assume that the excitations have the form of $\boldsymbol{F} = \boldsymbol{F}_0\sin(\omega t)$. If only the periodic motions are considered, the steady-state response is expressed as

$$x_i = \sum_{j=1}^{m} a_{ij}\cos(j\omega t) + b_{ij}\sin(j\omega t) \tag{41}$$

For simplicity, only the first two terms, which have the same harmonic with the excitation, are applied to calculate the response, that is,

$$x_i = a_i\cos(\omega t) + b_i\sin(\omega t) \tag{42}$$

The corresponding amplitude is

$$|x_i| = \sqrt{a_i^2 + b_i^2} \tag{43}$$

Introducing Eq. (42) into Eq. (16), (22), or (26) gives a set of simultaneous polynomials in the constants a_i and b_i. These nonlinear polynomial equations can be solved using the Newton–Raphson method.

Assume a unit force is acted on node 9 at the transverse direction. The amplitude-frequency relation curves (backbone curves) at nodes 9 and 30 resulted from the full global model are plotted

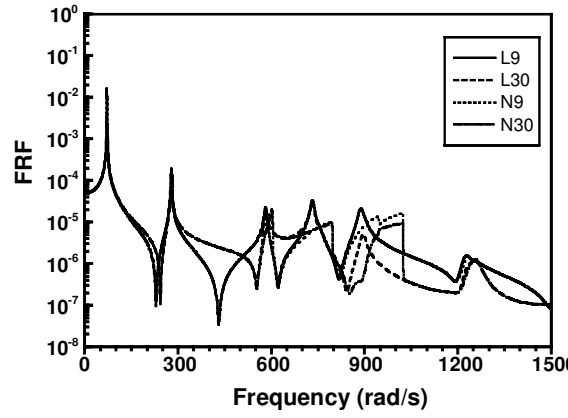

Fig. 3 FRFs with and without nonlinear springs.

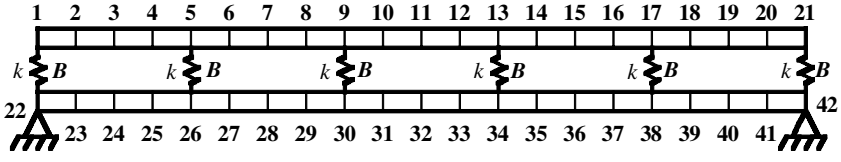

Fig. 2 Schematic of a beam-spring compound system.

in Fig. 3. In this figure L and N denote linear and nonlinear, respectively; 9 and 30 are node numbers. For simplicity, the jumps of the amplitudes are kept in these curves. Therefore, they are not exactly backbone curves. Although they are approximate, they will serve the purpose to check the accuracy of the reduced model. The transverse frequency response function (FRF) at nodes 9 and 30 for the system without nonlinear springs, indicated by L, is also plotted in Fig. 3 for comparison. In these four curves the proportional damping, $\boldsymbol{C} = 2 \times 10^{-5}\boldsymbol{K}$, is assumed for the two beams. For convenience the amplitude-frequency curves of the nonlinear system are also called FRFs.

At first, the model reduction scheme defined on the system level is used. The transverse DOFs at nodes 1, 5, 9, 13, 17, 21, 7, and 15 in the upper beam and nodes 22, 26, 30, 34, 38, 42, 28, and 36 in the lower beam are selected as the kept DOFs when the dynamic condensation method is applied. Hence, the reduced model has 16 DOFs including the two fixed ones. After the linear reduced model is available, the nonlinear springs are directly assembled to formulate the reduced global model. Again, the harmonic balance method is used to solve the nonlinear equations of the reduced model.

The FRFs of the reduced model at nodes 9 and 30 in the transverse directions are plotted in Fig. 4, respectively. The exact results are also plotted for comparison. In the following, if the FRFs obtained from the reduced model are very close to those from the full model we will say the reduced model can represent accurately the full model at that frequency range. The accuracy of the FRFs resulted from the initial approximation of the reduced model is very low especially for the FRFs at the high frequency range. With the increase in the number of iterations, the FRFs close to the exact solution quickly. The FRFs resulting from the second approximation, for example, are very close to the exact except at the jump around 1000 rad/s.

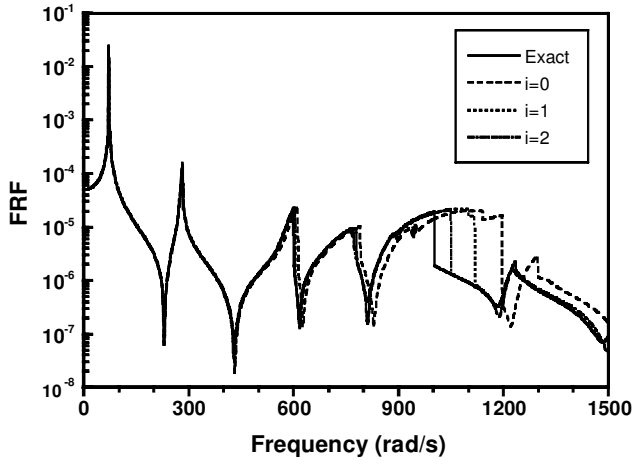

a) Node 9

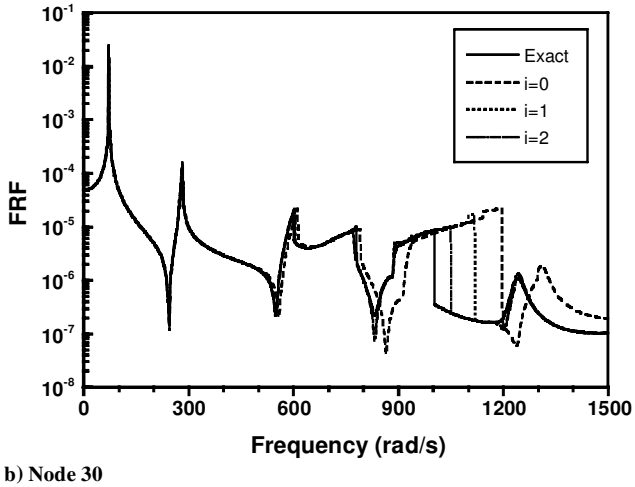

b) Node 30

Fig. 4 FRFs of the reduced model defined on the system level.

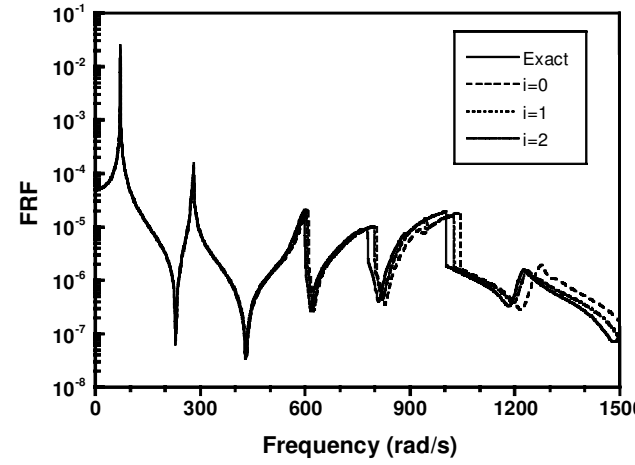

a) Node 9

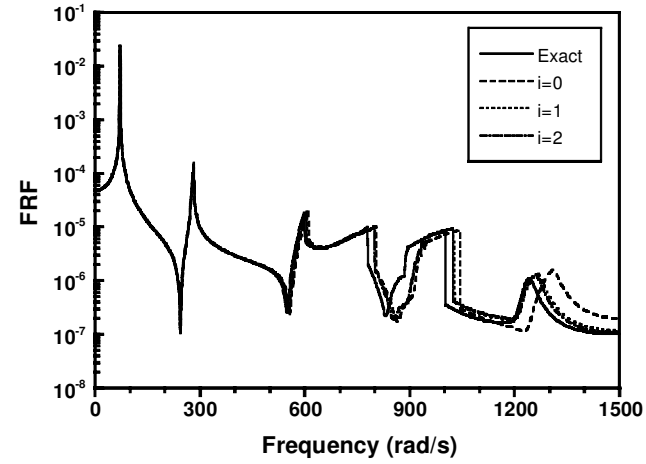

b) Node 30

Fig. 5 FRFs of the reduced model defined on the substructure level.

The reason for this discrepancy at this jump is that these curves are not exact backbone curves. Actually, the difference between the approximate FRFs with $i = 2$ and the exact is very small.

The two beams are selected as the flexible substructures when the model reduction scheme defined on the substructure level is used. The same kept DOFs are chosen for each beam. Because the two beams are identical, it is necessary to construct only one reduced model for the beams using the dynamic condensation technique. The system modeling scheme shown in Fig. 1 is used. The reduced global model has 16 DOFs including the two fixed.

Similarly, the FRFs of the reduced model at nodes 9 and 30 are plotted in Fig. 5. The exact results are also plotted for comparison. The accuracy of the initial approximation is low, especially for the FRFs at the high-frequency range, as shown in Fig. 5. With the increase in the number of iterations, the FRFs close to the exact solution quickly. The first approximation, for example, is much more accurate than the initial approximation.

The accuracy of the approximate FRFs resulted from the reduced model defined on the system level is a little higher than the reduced model defined on the substructure level. This phenomenon becomes obvious when $i = 1$ and 2, as shown clearly in Figs. 4 and 5.

For this example, 751 time step is used to simulate the FRFs of the full global model and the reduced global models. The code is run in a Sun 4500 computer with 400 × 8 MHz CPU, 4-GB memory. The computed time for the two models are 2999, 26 and 25 s, respectively. Clearly, the reduced model is much more computationally efficient than the full model.

Floating Raft Isolation System

For the second example, a floating raft isolation system[13] is considered. It contains springs, dampers, machines to be isolated, a

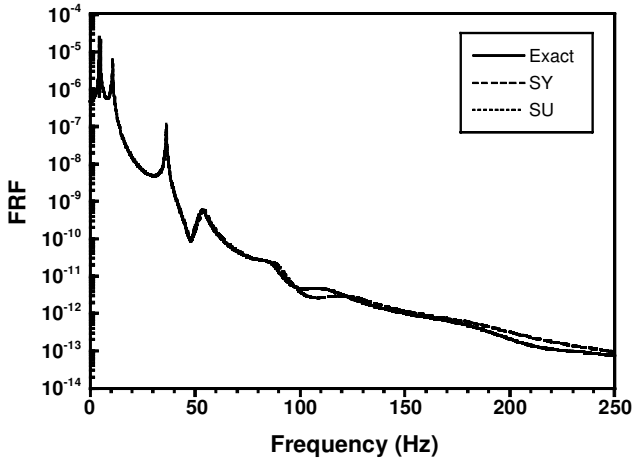

Fig. 6 FRFs of the floating raft isolation system.

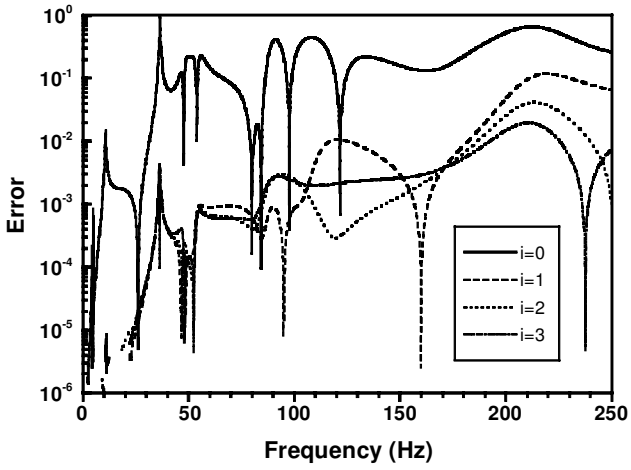

Fig. 7 Error of the FRFs of the reduced model defined on system level.

raft frame, and a base. It is very difficult to construct a reasonable dynamic model by using multi-rigid-body method or elastic wave analysis method when the raft frame and the base are a little complex, their elasticity are to be considered, and there are local nonlinearities.[9]

One spring with cubic stiffening nonlinearity, $B = 5 \times 10^{10}$ N/m^3, is mounted under masses 1 and 2, respectively. For both plates the damping is considered to be proportional to their stiffness matrices, and the ratio is 0.0003. The other parameters are identical to those in Ref. 13. The base and the raft are discretized by the finite element method. The base has 14 rectangular elements, 24 nodes, and 72 DOFs. The raft has 24 rectangular elements, 35 nodes, and 105 DOFs. Therefore, the full global model has a total of 167 DOFs except the fixed. Select the translational DOFs at m_1 and node 11 on the base as the input and output DOFs, respectively. The FRFs obtained from the full global finite element model are plotted in Fig. 6. They are considered as the exact for comparison purpose.

For the model reduction method defined on the system level, the translational displacements in the z direction at nodes 1, 3, 5, 7, 15, 17, 19, 21, 29, 31, 33, and 35 on the raft and nodes 7, 12, 13, 18, 8, 11, 14, 17, 9, 10, 15, and 16 on the base, and masses 1 and 2 are selected as the kept DOFs. The FRFs resulting from the initial approximation of the reduced model are shown in Fig. 6 and indicated by SY. The relative errors of the FRFs obtained from the reduced models with different approximations are plotted in Fig. 7. The accuracy of the FRFs obtained from the initial approximation is very low. Most errors are higher than 10%. When the iteration is applied, the errors are reduced very quickly. The maximum errors, for example, are reduced to 11.7, 4.1, and 1.9% after one, two, and three iterations are used.

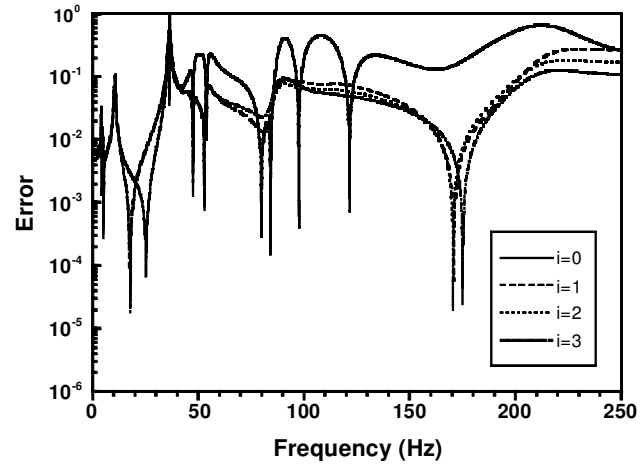

Fig. 8 Error of the FRFs of the reduced model defined on substructure level.

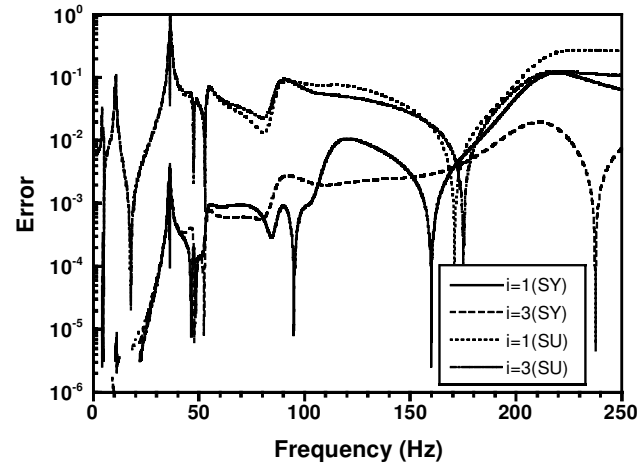

Fig. 9 Comparison of the errors from the two reduced models.

The two plates in the system are seen as two flexible substructures when the model reduction defined on the substructure level is used. The same DOFs on the two plates just used are selected kept DOFs. Both reduced models of the plates have 12 DOFs. Therefore, the reduced global model has 26 DOFs. The FRFs resulting from the initially approximate reduced model are also shown in Fig. 6 and indicated by SU. The errors of the FRFs obtained from the reduced models for different approximations are plotted in Fig. 8. Similarly, the errors of the initial approximate FRFs are very big. The error is reduced when the iteration increases, especially for the FRFs at the high-frequency range.

For this example, 2501 time step is used to simulate the FRFs of the full global model and reduced global models. The code is run in the same computer as just stated. The computed time for the two models are 1452, 6, and 6 s, respectively. The reduced model is much more computationally efficient than the full model. The current computer time is shorter than that in the first example although the number of DOFs of the present example is about double that of the first example. The reason is that the nonlinearity in the present example is much more localized than that in the first example. Consequently, more iterations are required in the first example.

The initially approximate FRFs resulting from the two model reduction approaches are very close, as shown in Fig. 6. However, the difference becomes clear when the iteration is applied. The errors of the FRFs resulting from the reduced models for $i = 1$ and 3 are plotted in Fig. 9. Clearly, the accuracy of the model reduction defined on the system level is much higher than the one defined on the substructure level.

Comparing the FRFs for $i = 0$ in Fig. 6 with those in Figs. 4 and 5, we find the accuracy of the former is higher than that of the latter two.

One of the reasons is that the nonlinearity in the second example is much more localized than that in the first example. Therefore, the present methods have higher accuracy for the system with local nonlinearities.

Conclusions

Based on the dynamic condensation technique, two model reduction approaches have been proposed in this paper. They are used to reduce the size of the large model with local nonlinearities before the analysis is performed on the global model. One is defined on the system level, and the other is on the substructure level. In the former scheme the dynamic condensation technique is directly implemented into the linear part of the whole system, whereas it is applied to the linear flexible substructures in the latter scheme.

As shown in the two numerical examples, the computational work can be reduced significantly by using the two approaches. Although some computational effort is required to construct the reduced model, this work is much less than the analysis of the nonlinear model directly and only required once.

The accuracy of the reduced models based on the initial approximation, Guyan condensation, is very low. When the iterations are applied, the accuracy increases very quickly. As shown from the examples, two or three iterations are usually enough for the accuracy.

The accuracy of the model reduction method defined on the system level is usually higher than that of the method defined on the substructure level, especially for the higher-order approximations. However, the former is more computationally expensive than the latter because the manipulation of larger matrices is required in the former approach.

References

[1]Zheng, T., and Hasebe, N., "An Efficient Analysis of High-Order Dynamical System with Local Nonlinearity," *Journal of Vibration and Acoustics*, Vol. 121, No. 3, 1999, pp. 408–416.

[2]Fey, R. H. B., van Campen, D. H., and de Kraker, A., "Long Term Structural Dynamics of Mechanical Systems with Local Nonlinearities," *Journal of Vibration and Acoustics*, Vol. 118, No. 2, 1996, pp. 147–153.

[3]Nataraj, C., and Nelson, H. D., "Periodic of Solutions in Rotor Dynamic Systems with Nonlinear Supports: A General Approach," *Journal of Vibration, Acoustics, Stress, and Reliability in Design*, Vol. 111, No. 2, 1989, pp. 187–193.

[4]Rouch, K. E., and Kao, J. S., "Dynamic Reduction in Rotor Dynamics by the Finite Element Method," *Journal of Mechanical Design*, Vol. 102, No. 2, 1980, pp. 360–368.

[5]Guyan, R. J., "Reduction of Stiffness and Mass Matrices," *AIAA Journal*, Vol. 3, No. 2, 1965, pp. 380.

[6]Mclean, L. J., and Hahn, E. J., "Unbalance Behavior of Squeeze Film Damped Multi-Mass Flexible Rotor Bearing Systems," *Journal of Lubrication Technology*, Vol. 105, No. 1, 1983, pp. 22–28.

[7]Shiau, T.-N., and Jean, A.-N., "Prediction of Periodic Responses of Flexible Mechanical Systems with Nonlinear Characteristics," *Journal of Vibration and Acoustics*, Vol. 112, No. 4, 1990, pp. 501–507.

[8]Qu, Z., and Fu, Z., "An Iterative Method for Dynamic Condensation of Finite Element Models, Part I: Basic Method," *Journal of Shanghai Jiao Tong University*, English ed., Vol. 3, No. 1, 1998, pp. 83–88.

[9]Qu, Z.-Q., "Structural Dynamic Condensation Techniques: Theory and Application," Ph.D. Dissertation, State Key Lab. of Vibration, Shock and Noise, Shanghai Jiao Tong Univ., Shanghai, PRC, Oct. 1998.

[10]Li, T. Y., Zhang, X. M., Zuo, Y. T., and Xu, M. B., "Structural Power Flow Analysis for a Floating Raft Isolation System Consisting of Constrained Damped Beams," *Journal of Sound and Vibration*, Vol. 202, No. 1, 1997, pp. 47–54.

[11]Yang, Y.-B., and Lin, B.-H., "Vehicle-Bridge Interaction Analysis by Dynamic Condensation Method," *Journal of Structural Engineering*, Vol. 121, No. 11, 1995, pp. 1636–1643.

[12]Berman, A., "Multiple Acceptable Solutions in Structural Model Improvement," *AIAA Journal*, Vol. 33, No. 5, 1995, pp. 924–927.

[13]Qu, Z.-Q., and Selvam, R. P., "Dynamic Superelement Modeling Method for Compound Dynamic Systems," *AIAA Journal*, Vol. 38, No. 6, 2000, pp. 1078–1083.

[14]Qu, Z.-Q., and Selvam, R. P., "Dynamic Superelement for Dynamic Systems with Local Nonlinearities," *Proceedings of the 42nd AIAA/ASME/ASCE/ASC Structures, Structural Dynamics, and Materials Conference and Exhibit* [CD-ROM], AIAA, Reston, VA, 2001.

[15]Lewandowski, B., "Computational Formulation for Periodic Vibration of Geometrically Nonlinear Structures—Part 1: Theoretical Background," *International Journal of Solids and Structures*, Vol. 34, No. 15, 1997, pp. 1925–1947.

A. Berman
Associate Editor